UNIVERSITY OF GAZIANTEP

GRADUATE SCHOOL OF

NATURAL & APPLIED SCIENCES

NEUTRON HALO AND RELATED STRUCTURE IN LIGHT NUCLEI

M. Sc. THESIS

IN

ENGINEERING PHYSICS

BY

LAKOUNDJI ROLAND RIPHAT GEOFFROY

JUNE 2017

Neutron Halo and Related Structure in Light Nuclei

M.Sc. Thesis

in

Engineering Physics

University of Gaziantep

Supervisor

Prof. Dr. Bülent GÖNÜL

by

Lakoundji ROLAND RIPHAT GEOFFROY

June 2017

REPUBLIC OF TURKEY
UNIVERSITY OF GAZIANTEP
GRADUATE SCHOOL OF NATURAL & APPLIED SCIENCES
ENGINEERING PHYSICS

Name of the thesis: Neutron-Halo and Related Structure in Light Nuclei

Name of the student: Lakoundji ROLAND RIPHAT GEOFFROY

Exam date: 16.06.2017

Approval of the Graduate School of Natural and Applied Sciences

Prof. Dr. A. Necmeddin YAZICI

Director

I certify that this thesis satisfies all the requirements as a thesis for the degree of Master of Science

Prof. Dr. A.Ramazan KOÇ

Head of Department

This is to certify that we have read this thesis and that in our consensus-majority opinion it is fully adequate, in scope and quality, as a thesis for the degree of Master of Science.

Prof. Dr. Bülent GÖNÜL

Supervisor

Examining Committee Members   Signature

Prof. Dr. Bülent GÖNÜL

Prof. Dr. Okan ÖZER

Assoc. Prof. Dr. Cumhur CANBAZOĞLU

I hereby declare that all information in this document has been obtained and presented in accordance with academic rules and ethical conduct. I also declare that, as required by these rules and conduct, I have fully cited and referenced all material and results that are not original to this work.

LAKOUNDJI ROLAND RIPHAT GEOFFROY

ABSTRACT

NEUTRON HALO AND RELATED STRUCTURE IN LIGHT NUCLEI

ROLAND RIPHAT GEOFFROY Lakoundji
M.Sc. in Engineering Physics
Supervisor: Prof. Dr. Bülent GÖNÜL
June 2017
37 pages

The works appeared recently dealing with exotic halo nuclei have displayed striking variations in nuclear shell structures and revealed the emergence of novel magic numbers unlike the stable nuclei. One of the significant reasons for these variations is the effect of tensor forces on nuclear structures, which has been reviewed in this report. Also, with the consideration of three-body nuclear forces, the known dramatic peculiarity over the oxygen isotopes has been debated to clarify why ^{24}O is the heaviest bound oxygen isotope. Finally, we focus at loosely bound neutron $s-$ states within the frame of light halo nuclei to grasp why the weak binding plays a crucial role in observing the change in energies of lowest states.

Keywords: Exotic nuclei, neutron-halo nuclei, $^{24}_{8}O$, nuclear tensor force, three-body interaction force, binding energy

ÖZET

HAFİF ATOM ÇEKİRDEKLERİNDE NÖTRON HALE YAPISI

ROLAND RIPHAT GEOFFROY Lakoundji
Yüksek Lisans Tezi, Fizik Mühendisliği Bölümü
Tez Yöneticisi: Prof. Dr. Bülent GÖNÜL
Haziran 2017
37 sayfa

Literatürde mevcut yeni çalışmalara göre, kararlı atom çekirdekleri bölgesinin uzağında yapılanan ekzotik çekirdeklere ait nükleonların bilinenden çok farklı enerji kabuk yapılarına sahip olduğu ve dolayısıyla ilgili enerji seviyelerinin yeni sihirli sayılarla açıklanabildiği anlaşılmaktadır. Bu tür atom çekirdeklerinin teorik analizinde, spin-izospin etkileşiminin diğer bir deyişle nükleer tensör kuvvetinin de dikkate alınması gerekliliği önemle vurgulanmaktadır. Ayrıca bir yeni bir de eski sihirli sayıya sahip ekzotik atom çekirdeğinin, ${}^{24}_{8}O_{16}$, bağlı duruma sahip en son oksijen izotopu olduğunun fiziksel izahında, valans nükleonlar arasındaki itici 3-cisim kuvvetinin de bu tür teorik analizlerde içerilmesinin gerekliliği ileri sürülmüş ve ilgili alanda bir başka devrim yaşanmıştır. Tüm bu yeni düşünceler, tez çalışması kapsamında dikkatlice gözden geçirilmiştir. Yine bu çerçevede, hale yapısı içeren ekzotik hafif atom çekirdeklerine ait zayıf bağlı valans nötron S-dalgalarının literatürde mevcut deneysel sonuçlar ışığında teorik modellemesi incelenmiş ve bağlanma enerjisi ile hale parçacıklarına ait durum dalgalarının değişimi arasındaki ilişki araştırılmıştır.

Keywords: Ekzotik çekirdekler, nötron-hale çekirdekler, ${}^{24}_{8}O$, nükleer tensör kuvveti, 3-cisim etkileşim kuvveti, bağlanma enerjisi.

ACKNOWLEDGEMENTS

TABLE OF CONTENTS

LIST OF FIGURES

LIST OF SYMBOLS/ABBREVIATION

N: Neutron number

Z: Proton number

$^{6,7,8,9,10,11}_{3}Li_{3,4,5,6,7,8}$ **:** Lithium isotopes

$^{208}_{82}Pb_{126}$ **:** Lead

$^{11}_{4}Be_{7}$ **:** Beryllium

$^{30}_{14}Si_{16}$ **:** Silicon

$^{16,22,24,28}_{8}O_{8,14,16,20}$ **:** Oxygen isotopes

$^{40}_{20}Ca_{20}$ **:** Calcium

He: Helium

β **:** Beta-decay

ℓ **:** Orbital angular momentum

MeV: Megaelectronvolt

SPEs: Effective (spherical) single particle energies

$\hat{V}$ **:** Two-body interaction

j and j' **:** Single particle orbits

k and k' **:** Magnetic substates

$\left\langle ...|\hat{V}|...\right\rangle$ **:** Two-body matrix elements

s, p, d, f, g : Nuclear subshells

$\vec{\tau}_{1,2}$ **:** Isospin interacting nucleon

$\vec{s}_{1,2}$: Spin of interacting nucleons

. : Scalar product

$f(r)$: radial function for interacting two particles

T $\left(\left(\dfrac{(N-Z)}{2} \leq T \leq \dfrac{(N+2)}{2}\right)\right)$ **): Isospin**

V_0 : Potential strength

V : Potential

ΔV : Potential variation

E_n : Neutron energy

$\Delta E \exp$: Experimental variation energies

ΔE : Energy variation

fm : Fermi

V_c : Central potential

V_C : Coulomb potential

$r(=\vec{r}_1 - \vec{r}_2)$: Distance between two nucleons

V_{SO} : Spin-orbit potential

$V_0(r)$: Spin independent central potential

R_c : Coulomb radius

R_0 : Nuclear radius

CHAPTER 1

INTRODUCTION

The investigation of nuclear structure for nuclei around the driplines is nowadays one of the significant and attractive fields in physics. Within this context, the motivation behind the present thesis work is to make an overview of the exotic nuclear shell structure of these dripline nuclei, together with features of specifically chosen loosely bound $S-$state neutron-halo nuclei, being away from the region of stability line. The peculiar features of such nuclei have been discovered recently, which directly resulted to leave the well known magic numbers for the nuclear structure investigations of newly discovered like nuclides, and the physics behind these structural interesting changes has been in turn studied carefully in the literature, which is one of the other subjects of the present work. In fact, the physics of interest for these structural changes under consideration has not yet completely cleared out and leads therefore to novel investigations and challenges. Nevertheless, this report presented here makes a proper summary of the reliable works published more recently, regarding the topic underlined, in the related literature considering many properties of the internucleon interactions, among them the spin-isospin/tensor terms, together with 3-body forces, play decisive roles in such evolutions as well discussed through the present work.

Before 1934, physicists focused the existence of some specific numbers of nucleons which indicate for the nucleus of interest some definite stable energy levels for neutrons and protons. In similar to electrons in atoms, physicists related these specifically considered numbers with closed shells for nucleons in nuclei moving around energy levels due to properly chosen a confining potential form. After some time, the search for the shell structure re-attracted the attentions of some leading

nuclear scientists, causing to new considerable amount of reliable data, which clarified that stable nuclei have fully filled up shells at these magic numbers such as 8, 20, 50, 82 and 126. Later, with the involvement of spin-orbit force interactions in their calculations, researchers illuminated the observed gaps between the shells. The reader is referred to the next chapter for a further reading and progress on this subject. Simultaneously all these specific numbers were recalled as the magic numbers through with many systematics in those days were able to clarified in detail. This exploration then greatly enlightened in revealing, in appropriate form, the nuclear structure and these magic numbers became the backbone of the advanced researches in nuclear structure physics. Thus, these magic numbers settled down as a dogma in nuclear physics for a long time.

With the increase in experimental techniques for discovering exotic nuclei with relatively large N/Z ratios, the permanence of these magic levels for some nuclei not closed to stability line was first broken for $N = 20$. The related experimental investigations obtained in those days have obviously clarified that the $N = 20$ gap in between energy shells was quite breakable for nuclei far from stability, which is well discussed through the next chapter.

Since then, many facilities based on radioactive ion beam have appeared all around the world and overwhelmingly physicists believed that new magic numbers may naturally appear when the case such as an extreme proton-to-neutron ratios are observed. The properties of these shell gaps around the stability line have served to improve and suggest new physically meaningful sophisticated quantum mechanical appropriate models.

Apparently, the strong belief in the old usual magic numbers has struggled in theoretical nuclear physics for considerably long time, till the beginning of investigations for exotic nuclei having extreme N/Z ratios. Along this line, so many interesting works in the literature, which well discussed through the next chapters,

testing the reliability of the usual shell closures and understanding the physics behind the appearance of new shell structures, have been emerged. These remarkable scientific novel approaches have analyzed carefully the related data accumulated for exotic halo nuclei to be able to clear out the mentioned structural novel evolutions and the reveal of novel magic numbers, within the frame of significant features of the nucleon-nucleon forces with in particular the tensor term and 3-body forces unlike the previous stable nuclei considerations.

Within this frame, the whole of the subsequent chapters have been devoted to a deep understanding of the neutron-halo structure for light exotic nuclei involving the effects of the nuclear forces concerning with especially its tensor/spin-isospin part and of the three-body repulsive nucleon-nucleon interactions, together with the contribution of the weakly binding halo nucleon to the disappearance of the traditional magic number while a novel shell structure appears with a new magic number due to the exotic structure of halo nuclei.

CHAPTER 2

SHELL EVOLUTION FOR LIGHT NEUTRON HALO NUCLEI

2.1. Theoretical Background

The quantum halo structure based on nuclear physics arises for exotic systems where the corresponding radii are significantly larger than that of the nuclear force, unlike the similar systems related to stable nuclei. More specifically, neutron (proton) halo structure has an extreme extension for the related radial wavefunction having a weak bound for halo particles due to their tunneling outside of the nuclear force interaction range. These exotic nuclei first introduced via the observations of Tanihata *et al* [1,2] on nuclear sizes of halo nuclides and called, after a few years, as neutron halo by Ref. [3], where the properties of their structure was discussed in detail. For instance, the two isotopes $^{6,7}_{3}Li$ of lithium atom are stable. Through the addition of neutrons, one handles $^{8,9}_{3}Li$ being as bound due to attraction of nuclear interaction, nevertheless they disintegrate, after in a very short time duration, through β-process. For the other isotopes of this atomic nucleus having larger neutron numbers, the binding energies of valance neutrons decrease quickly. However, it is quite interesting that the strength of the nuclear interaction force for $^{10}_{3}Li$ is not enough to make a binding for the last neutron. But in case of $^{11}_{3}Li$, the situation is different because the whole system involving the halo di-neutrons is bound. In spite of a tiny binding energy, this nucleus has been observed as bound because of the correlation between the last two neutrons in $^{11}_{3}Li_{8}$, but it also decays through the β-process, depending on its half-life, like its other isotopes. There is an interrelation between this tiny binding energy of the nucleus and the weak binding of the valance two halo neutrons as the resultant wave functions tunnels beyond the range of nuclear forces as pointed out in Ref. [3], which will be the subject of Chapter 3. At this stage, it should be

emphasized that the size of $^{11}_{3}Li$, due to the exotic structure mentioned, is close to that of the heavier nucleus ^{208}Pb . Though this explanation here seems very natural and understandable at present, a long time elapsed before the acceptation of this physics underlined through the related scientific community.

Quantum halos have introduced a significant contribution to the literature, which triggered many other interesting investigations since then, see for example [4–14]. The most decisive feature of a neutron halo, as mentioned earlier, is the tunneling of the corresponding wavefunction beyond the potential well because of the loose binding of halo neutrons having in particular $\ell = 0$ angular momentum. The system hence can then be splitted into a core and halo neutrons which enable for tunneling out of the related nuclear force, describing a halo structure. For instance, the well known neutron halos discovered at earlier stages, such as ^{11}Li and ^{11}Be , together with the others involving two- and three-body halo nuclei in Tables 2 and 3 of Ref. [15], are the good examples for such an exotic structure, unlike stable nuclei, bearing in mind sufficiently small binding energies of such exotic structures having less than about $1\,MeV$ or more precisely less than $2MeV\,A^{-2/3}$ [3]. Nevertheless, there is as yet no clear answer to where, in what size of nuclei, nuclear halo state occurs. At present, considering the experimental and theoretical findings concerning with such nuclei, the main consensus on that is the nuclear halos largely emerge in the ground states or at lowest energy levels and thus this observation justifies the dripline physics. For a more comprehensive discussion on this topic the reader is referred to [13,15,16].

In connection with this, as being the newly most popular research area in nuclear structure physics, the physicists have focused at specifically the new concept of single-particle energies (SPEs) for dripline nuclei in the light of new forms of their shell structure for exotic nuclei, and even at dramatic changes in the traditional magic numbers of stable nuclei, which are the subject of the next section.

2.2. Exotic Nuclei and Nuclear Force

The present report makes an overview on novel appearance of the nuclear structure concerning with neutron halo nuclei in comparison with stable atomic nuclei, considering some significant characteristic effects of nuclear interactions. As is well known [17,18], the shell structure of nuclei has been helpful for a long time as a physically meaningful framework for nuclear physicists in grasping the mutual motions of nucleons including its strong validity for the whole of stable atomic nuclei with the familiar numbers, 2, 8, 20, 28, 50, ... Consequently, this belief emerged a reliable and powerful calculation framework, involving a central with spin-orbit interaction forces, for the corresponding energy levels of nucleons moving in a closed shell with these magic numbers. Keeping in mind that the known traditional magic numbers used for stable nuclei cause a strong binding, these numbers however are fragile when nuclei approach around the driplines. This disappearance of conventional numbers is certainly concerning with the exotic dripline nuclei due to their novel nuclear halo structure having highly asymmetric neutron/proton ratios. Within this context, the physics behind this peculiar halo structure have been recently discussed in detail through the properties of nuclear forces [19, and the related references therein] and clarified that new shell structures occur in different perspectives as more nucleons are added to the isotopes. The key points of this *shell evolution* particularly through the few-body nuclear interactions are one of the motivations behind the work presented in this report. The following sections, in the light of the recently published experimental results, illuminate clearly that novel numbers for specific shells emerge and a new forms of shell structures appears for the nuclei under consideration. Namely, in the other words, traditional shell gaps for atomic nuclei disappear whereas surprisingly some new gaps between the nucleon energy levels are seen to appear instead.

In these calculations mentioned above, three types of nuclear forces have been dominantly considered. The first significant one is the tensor force which are capable

for changing the spin–orbit splitting for a specifically chosen orbit. This results of course in variations of the nuclear shells in exotic nuclei, and, as a result of this, some of conventional *magic numbers* disappear while the alternative numbers appear, which will be discussed in detail below. The other significant nuclear force,   for the analysis of halo structures, is the one called central interaction forces. Otsuka [19] has recently clarified that yet uncovered properties of the central force used in the Hamiltonians within the framework of theoretical models can yield nuclear structures in agreement with experimental findings due to its significant effect on the shell evolution. The third one of an appropriate nuclear force consideration, required for the reliable analysis of exotic nuclei, is the inclusion of a three-body interaction in such a shell structure that reproduces a repulsive interaction between the weakly bound halo neutral particles moving beyond the core and the third one in the latest shell of the core [19]. In particular, the consideration of 3-body interaction forces in the related Hamiltonian, cause a strong prediction for defining the physically acceptable dripline region in a well agreement with the observations for new exotic oxygen isotopes, such as $^{24}_{8}O_{16}$, which is another interest of the present work. Hence, the domain of atomic nuclei takes place in between stable to exotic ones due to specific consideration of nuclear interactions, causing to an amazing enlargement in the nuclear chart.

For more than a quarter century, however, the primary interest of the physics within the frame of nuclear structure has been driven from stable nuclei to the new domain called exotic nuclei. As is now well known, exotic nuclei have quite short life times and they have large neutron numbers when compared to those of protons, unlike the stable ones.
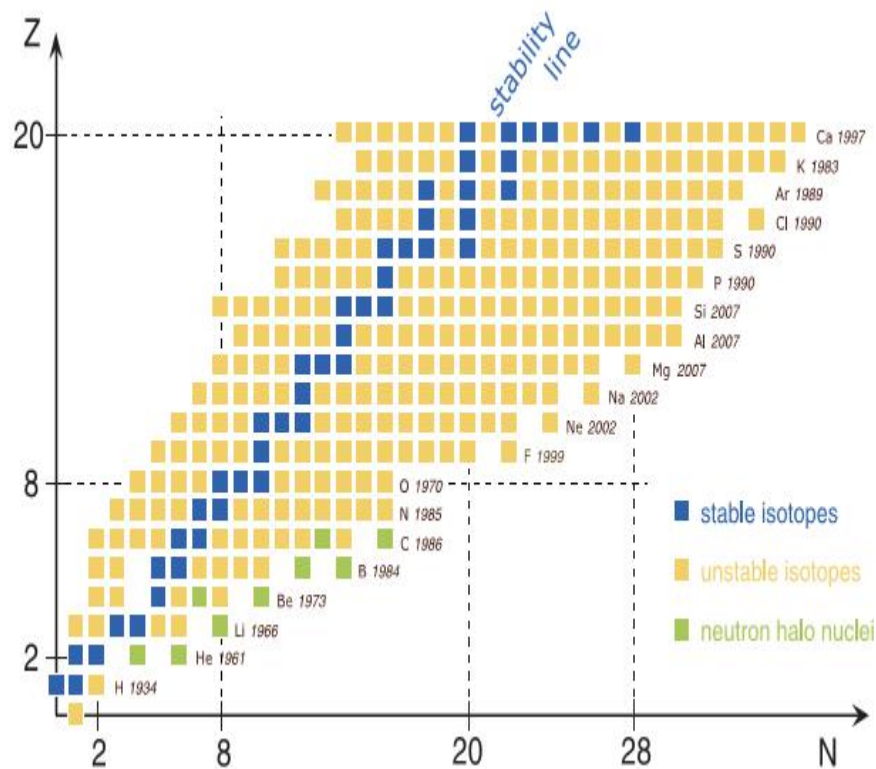
Fig. 1. The related part of the nuclear chart. Taken from [19].

Fig.1 illustrates some well known neutron halo nuclei, together with others. Clearly, there is a borderline, called as the *neutron drip line* in the literature, beyond which there is no possibility to observe a bound isotope through the additional neutrons. Apparently, the neutron halo structure is a natural consequence of exotic nuclei around the drip line, which is obviously one of the great improvements in nuclear structure physics based on radioactive ion beam technology leading to many

interesting theoretical and experimental researches. In Fig. 1, stable nuclei (blue squares) shape a line on the associated nuclear region. Though this is not an excellent steady line, this clustering of stable nuclei is known as the *β-stability line*. The neutron drip line at present exists in the related domain up to oxygen isotopes ($Z = 8$). On the further side of this point, the dripline for neutral particles is not sufficiently understood, and one naturally expects at this stage that it should go beyond the rightest isotopes in Fig. 1.

The first step in understanding the effects of nuclear interactions on the shell evolution is to start with the monopole component of a given two-body interaction, $\hat{V}$. More specifically, in grasping single particle properties underlined for a nucleus, one uses *effective (spherical) single-particle energies* (ESPEs*)*, which represent average effects from the other nucleons on a nucleon in a specified single particle orbit. The two-body matrix element of the interaction depends on the quantum numbers coupled by two interacting nucleons. We therefore first define the monopole matrix element of this two-body interaction, $\hat{V}$, as

$$v_{m;j,j'} = \frac{\sum_{k,k'} \left\langle jkj'k' \left| \hat{V} \right| jkj'k' \right\rangle}{\sum_{kk'} 1} \tag{1}$$

where j and j' represent interacting single particle orbits. Here k and k' are their associated magnetic substates and $\left\langle ... \left| \hat{V} \right| ... \right\rangle$ is the related two-body matrix element. Eq. (1) denotes an averaging over all feasible states of two interacting nucleons. In the other words, the monopole component of the interaction implies the mean effects of $\hat{V}$ depending solely specific quantum features of the interacting nucleon states [19,20]. The ESPE is evaluated from this Hamiltonian as an average effects from the other nucleons. In general, the ESPE of an *occupied* orbit is defined to be the separation energy of the related energy level with the opposite sign. Note that the separation energy yields the minimum energy required to separate a nucleon from this orbit. Whereas the ESPE of an *unoccupied* level is described to

be the binding energy gained by adding a nucleon to this energy level with the opposite sign.

With this consideration, the variations in the nuclear shells, called *shell evolution*, in exotic nuclei through the nuclear interactions was argued first in Ref. [21] considering the possible effects of loose binding on the nuclear shell structures. Figs. 2-a and 2-b, taken from [21], clarify in an explicit form the variation in the corresponding shells for the stable ^{30}Si nucleus and the exotic ^{24}O one, both of which have the same neutron numbers $N = 16$. In the usual treatment, six protons occupy $0d_{5/2}$ levels in ^{30}Si, whereas no proton is there in ^{24}O nucleus. The mentioned monopole interaction between protons moving in $0d_{5/2}$ shell and neutrons in $0d_{3/2}$ is strongly attractive, and causes to the striking difference between the Figs. 2 (a) and (b), where the old conventional *magic number N = 20* is replaced by 16.
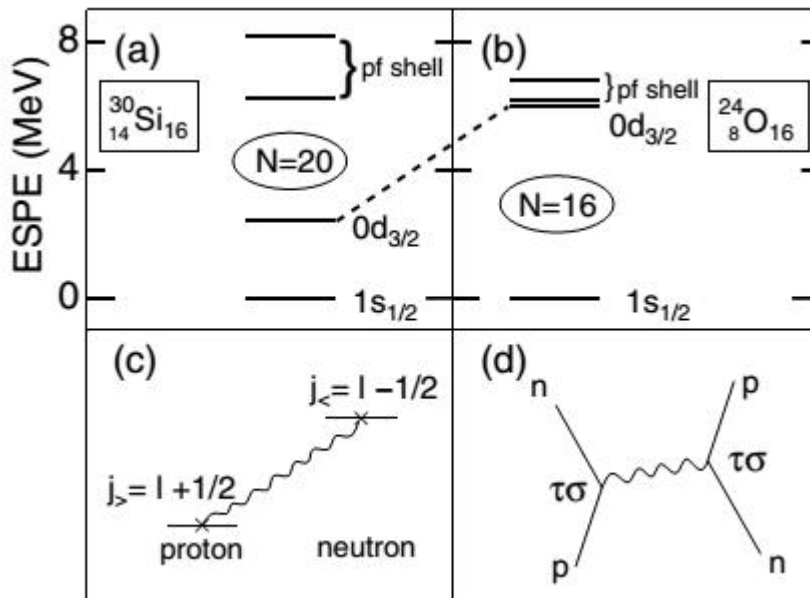
Fig. 2. Neutron effective single particle energies for (a) ^{30}Si and (b) ^{24}O, relative to $1s_{1/2}$. Reprinted from [21].

The detail discussion on the origin of the change underlined was given in [21]. It was concluded that the emphasized force is the piece of the tensor force, known as *spin–isospin* interaction due to the coupling between proton in $0d_{5/2}$ and neutron in $0d_{3/2}$ orbits mentioned above. A simple such an interaction was considered in detail by [21], which was a central force depending on spin (also see [22], together with Appendix A),

$$V_c = (\overline{\tau}_1.\overline{\tau}_2)(\overline{s}_1.\overline{s}_2) f(r) \tag{2}$$

where $(\overline{\tau}_{1,2})$ and $(\overline{s}_{1,2})$ represent the isospin and spin, respectively, for interacting nucleons, and the symbol $(.)$ denotes a scalar product. Here, *f(r)* is an r – dependent radial function for interacting two particles. More detailed advanced investigations clarified, however, that this calculation technique *is not appropriate*, while the component in Eq. (1) is physically acceptable. A proper understanding of Fig. 2 has been so far known to be handled by altering the spin-dependent-central interaction in Figure 2 (d) with *tensor force, namely, spin–isospin interaction*. Thus, despite the opinion put forward by [21], regarding the strong monopole interaction and resultant changes in shell structures, was a significant step in nuclear physics, the physicists had to wait until 2005 *for a clear understanding the related picture,* when the *shell variations by the tensor force* was explicitly clarified, which will be discussed in following section.

## 2.3. Tensor force and shell evolution

Here, we discuss the physics behind the changes in the nuclear shell structure due to the tensor interaction. The meson exchange process of the nucleon-nucleon interaction proposed first by Yukawa and its significant piece due to tensor force is one of the important effects enabling the variations systematically in single particle energy levels of nucleons.

In the usual shell-structure picture suggested in 1949 [17,18] one of the incompleted parts is the lowest order contribution of the tensor interaction force. In fact, pion exchange process within the frame of the nuclear forces mainly creates the tensor force, and more than one pion exchange produces the strong central force. In general, it is well known that vast of nuclear binding is because of this central force [23]. In reality, effects of the tensor force have automatically been involved in numerical results, but its broad features have not been reported in a proper form up to the work performed by [24], where the *variation in the nuclear shells* due to the tensor interaction was presented for the first time.

Considering the comprehensive discussion in [24], we begin with cases like Fig. 3 with orbital angular momenta being denoted by ℓ or, ℓ', protons are in either $j_> = \ell + 1/2$ or $j_< = \ell - 1/2$ while neutrons are in either $j'_> = \ell' + 1/2$ or $j'_< = \ell' - 1/2$.
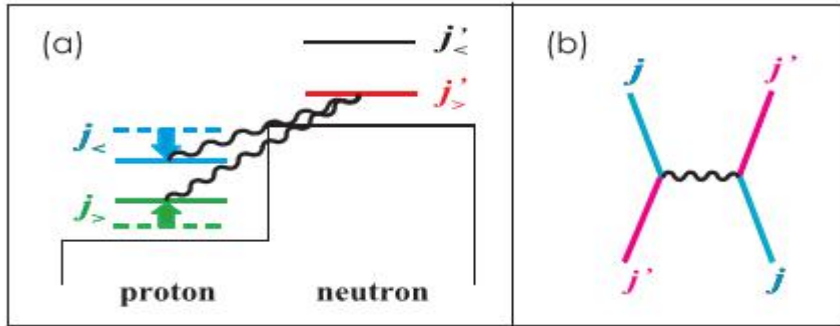
Fig. 3. (a) Tensor interaction between a proton in $j_{>,<} = \ell \pm 1/2$ and a neutron in $j'_{>,<} = \ell' \pm 1/2$. (b) Exchange processes. Reprinted from [24].

The question at this stage is the understanding of the effects through the tensor interaction in evaluating single particle energies (ESPEs). The answer is given in [19] by an intuitive frame. Fig. 4 (a) denotes the situation with a nucleon on $j_<$ is in the mutual interaction with another on $j'_>$ via the tensor forces. The sum of the spins

should be $S = 1$. The motion of orbits of two nucleons then should be in different directions as shown in Fig. 4 (a) similar to the bound deuteron case.
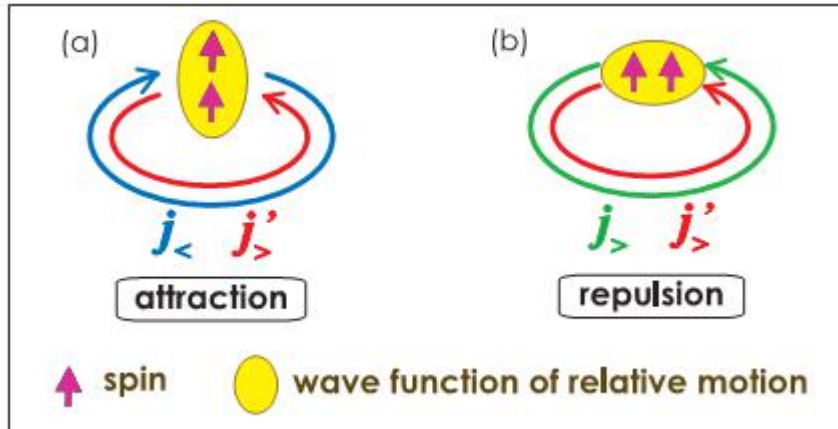
Fig. 4. Schematic representation of tensor force interaction for two neutral particles. Reprinted from [24].

More clearly, $j_<$ and $j'_>$ states attract each other, unlike $j_>$ and $j'_>$ case where they repel each other. This two-body interaction predicts also the binding energy being proportional to the number of particles in the orbital of interest. The $j_>$ orbital is less and less bound when the number of neutrons in the $j'_>$ orbital increases. On the other hand, the $j_<$ orbital is more bound for a larger number of neutrons in the $j'_>$ orbital. The energy gap between $j_>$ and $j_<$ orbitals, therefore, varies if the number of neutrons changes, providing a mechanism of changing spacing between single-particle orbitals. Thus, this simple intuitive explanation clarifies in an obvious way the shell structure evolution due to the tensor force. Further, considering Eq. (1) for the states j and j', the expression below is also valid for the tensor force as

$$\left(2j_> + 1\right)v^T_{m;j_>,j'} + \left(2j_< + 1\right)v^T_{m;j_<,j'} = 0 \tag{3}$$

in which the isospins $T = 0$ and 1, and j' is being either $j'_>$ or $j'_<$. Note that this equality appearing in the isospin formalism is applicable not only to cases like in Fig. 3 (a) but also to the situations between neutrons or between protons separately. Eq. (3) suggests that if both $j_>$ and $j_<$ levels are closed, their total tensor monopole effect diminishes, as in the $\ell = 0$ case.

Moreover, Fig. 5 indicates neutron single particle energies (SPEs) around N=20 for Z=8-20. At Z=8, one sees the evolution of the N=20. While the change is monotonic without the tensor force, the tensor force produces a sharp widening from Z=8 to 14, like the case in Fig. 2(a) and (b), and then stabilizes the gap towards Z=20. It is worth mentioning that the normal SPEs arise at Z=20 with the N=20 gap size as large as =6 MeV, whereas at Z=8 the inversion between $f_{7/2}$ and $p_{3/2}$ occurs and $d_{3/2}$ is rather close to $p_{3/2}$, leaving the major gap at N=16 as large as =5MeV. The central force lowers the neutron $d_{3/2}$ SPE more than the $f_{7/2}$ SPE as protons occupy the sd-shell due to larger overlaps, yielding a wide N=20 gap at ^{40}Ca. The N=20 gap at Z=14 is, however, largely due to the tensor force. For details see Ref [19].
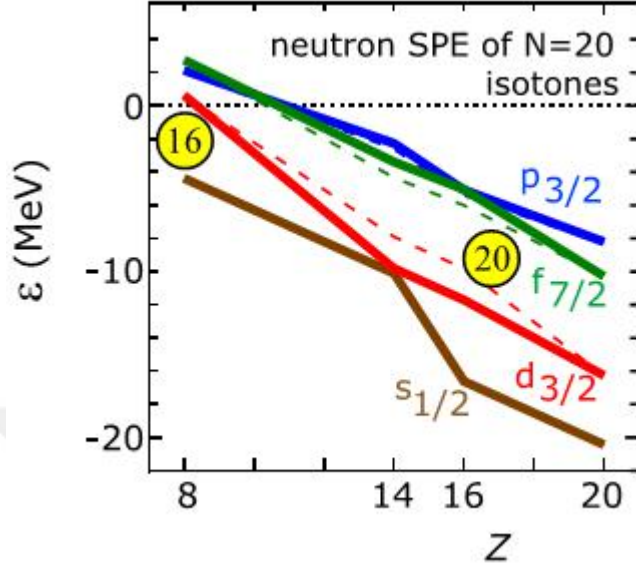
Fig. 5. Neutron single particle energies. The dashed lines denote the calculations with the central force only whereas the solid lines involve both the central force and the tensor force. Taken from [19].

Fig 5 once more justifies that the whole discussion given above regarding the effects of tensor force on the nuclear shell structures.

2.4. Effects of Three-body Force for ^{24}O

We now focus on to another major topic, the effects of three-body force, based on [25]. Fig. 1 clarifies that the neutron drip line emerges naturally with the increase in proton numbers. The only striking peculiarity exists in the oxygen isotopes, where the drip line is interestingly close to the stability line [26]. In this section we discuss this puzzle, along the work in [19], and show the strong requirement of three-body forces to explain why the doubly-magic $^{24}_{8}O_{16}$ nucleus [27] is the heaviest bound oxygen isotope.

We first try to understand why this oxygen anomaly is not appeared in usual shell-model calculations, which performed *without* three-body interactions, derived from microscopic nucleon-nucleon interactions. This can be clarified through the start from the stable ^{16}O nucleus and adding neutrons into the nucleon orbitals above the ^{16}O core by the assumption [19] that correlations do not change this intuitive picture. In this case, neutrons occupy first the $0d_{5/2}$ energy levels, with a closed shell alignment at ^{22}O ($N = 14$), then the $1s_{1/2}$ levels at ^{24}O ($N=16$), and finally the $0d_{3/2}$ orbital at ^{28}O ($N = 20$). In Fig. 6, which is taken from Ref. [19] based on the reliable calculations within the frame of effective field theory, the corresponding single particle energies of the neutron for $d_{5/2}$, $s_{1/2}$ and $d_{3/2}$ orbitals at subshell closures $N = 8, 14, 16$ and 20 are shown. For these energy values based on NN forces in Fig. 6 (a), the $d_{3/2}$ orbital go down rapidly as neutrons linger around the $d_{5/2}$ level, and remains well bound beyond $N = 14$. This leads to bound oxygen isotopes out to $N = 20$ and puts the neutron drip line *in a wrong place* at ^{28}O, leading to unphysical expectations.
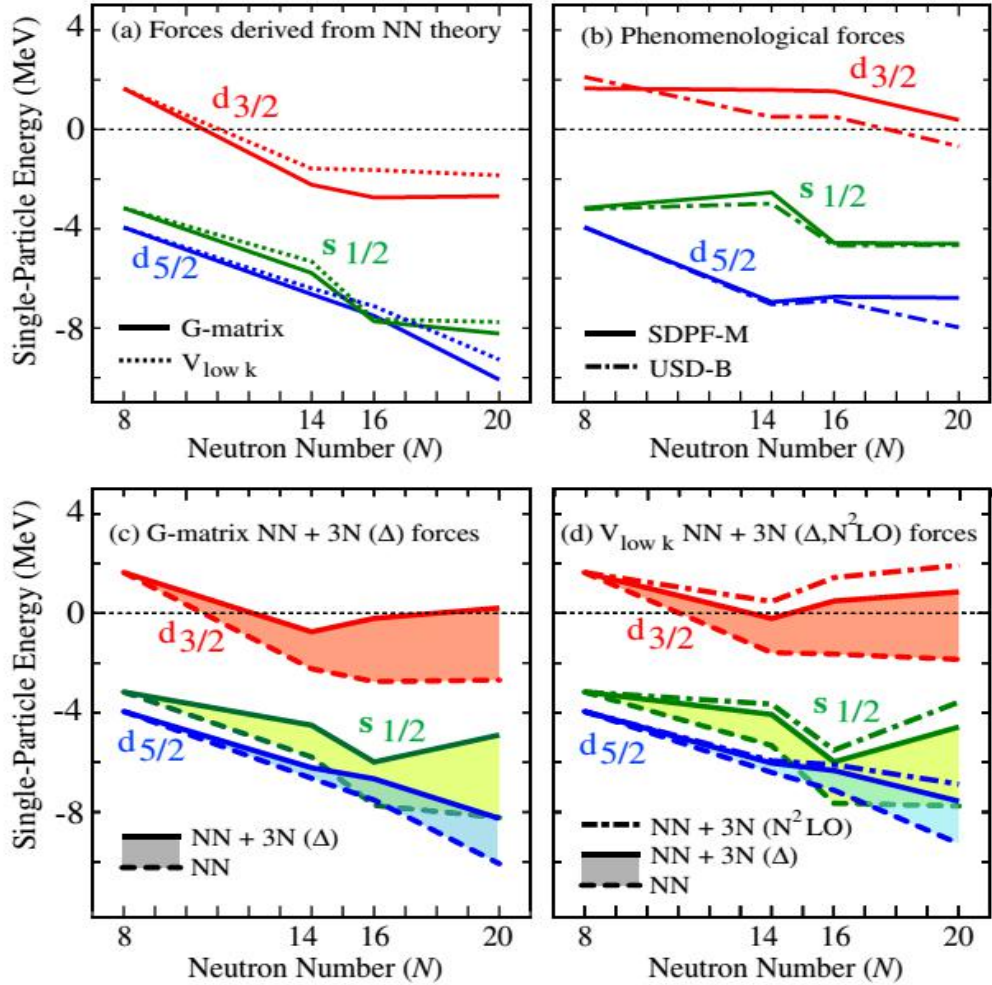
Fig. 6. Panel (a) presents the SPEs calculated by [28] and [29]. Panel (b) shows the SPEs obtained from the phenomenological forces by [30] and [31]. The contributions from 3N forces by chiral interactions carried out by [32] which are included in panels (c) and (d). Reprinted from [19].

For the clarification of the oxygen peculiarity, *we now focus* on Fig. 6 (b) in which the single particle energies obtained by the phenomenological forces [30] and [31] that have been fit to *r experimental data*. This shows a *striking difference* compared to Fig. 6 (a) *as neutrons occupy* the $d_{5/2}$ orbital, with N changing from 8 to 14, the $d_{3/2}$ orbital remains *almost* at the same energy and is *not well-bound* out to $N = 20$.

The *dominant differences between* the microscopic results of Fig. 6 (a) and those obtained from *phenomenological forces*, Fig. 6 (b), can be traced to the monopole components of two-body interaction (see Eq. (1)). *The comparison* of Figs. 6 (a) and (b) *suggest that* the monopole interaction between the $d_{3/2}$ and $d_{5/2}$ orbitals obtained from the microscopic theoretical models underlined is *too attractive*, and that the oxygen anomaly can only be solved by *additional repulsive contributions* to the two-neutron monopole components, which *approximately cancel* the average nucleon-nucleon attraction on the $d_{3/2}$ orbital. We also note that *3N forces* arise because nucleons being as composite particles have finite mass that *can be excited* by interacting with other particles. As is clear from this short discussion, and from the figure below taken from [25], that *three-body nucleon interaction between two valence neutrons beyond the core and one nucleon in the* ^{16}O core give rise to repulsive monopole interactions between the valence neutrons.
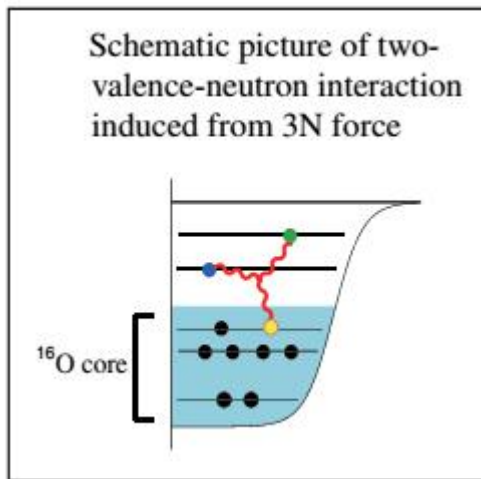
This repulsive contributions revealed elegantly by *3N forces* among excess neutrons lead obviously a *striking change* for the location of the neutron drip line from the theoretically (*misleadingly*) expected ^{28}O to the experimentally observed ^{24}O that is the *most neutron rich bound isotope of oxygen* around the drip line. This also can be easily understood from Fig. 7 (a) in which a large shell gap between $1s_{1/2}$ and

$0d_{3/2}$ at neutron rich $N = 16$ brings the $0d_{3/2}$ orbital higher up and, thus, this orbital is unbound in oxygen isotopes beyond ^{24}O. Overall, from this short but intuitive discussion, it is obvious that *3N forces* play indeed a key role for magic numbers in exotic nuclei and they are *directly responsible* in enlarging the $N = 16$ gap between the $s_{1/2}$ and $d_{3/2}$ orbitals [34]. This few-body force under consideration appears also in neutron stars and the other exotic nuclei in a similar mechanisms with, however, a high density in the former but a lower one in the latter.

In summary, the last years testified a new revolution in our view of the atomic nucleus in the exotic region. The β – unstable exotic nuclei situated far away from the stability line have changed our well established traditional concepts of the nuclear shell structure. Along this line, in Sections 2.1 and 2.2, we have presented the importance of the monopole interaction together with the tensor, central and three-body forces in analysing such nuclei. The whole review in Chapter 2 has explicitly clarified that the consideration of such forces in theoretical analysis of halo nuclides produces obviously a required striking shift in evaluating the related shell structure at novel magic numbers. The discussions presented in the above sections are also in agreement with [38] as tensor interactions as well as three-body interactions are particularly important for the binding of light nuclei. This intimates novel regions of the nuclear structure in entering borders of exotic nuclei. Beside these points, the effects of also the pairing interaction and weak binding are vital for the analysis of exotic shell structures, which is the subject of the next section. Perhaps many other unknown effects yet to be uncovered.

CHAPTER 3

NEUTRON *S*-STATES IN LOOSELY BOUND NUCLEI

From the discussions in the previous chapter, it is now obvious that the nuclei located around the dripline, having an increase in neutron numbers when compared to their isotopes, have valence halo neutron(s) with a tiny binding. Consequently, the corresponding neutron separation energies gets weaker leading to a considerable variation in the diffuseness of the densities due to these neutrons at the surface of the nucleus. This highly diffuse radially extended tail in the form of a nuclear halo emerges in this case. This unusual structure is concerning with the variations in nuclear levels of nucleons diverging dramatically from our traditional knowledge as referred above. This halo structure is in particular appears for orbitals having lower angular momenta (such as $1s_{1/2}$) with loosely bound neutrons. Fig. 7 (a) shows the orbitals for neutral particles obtained by a Woods–Saxon potential form [34], see Appendix B. It is clearly observed that in the domains of quite small neutral particle separation energies the $1s_{1/2}$ orbital *comes lower down crossing* the $0d_{5/2}$ level because of halo formations. This can be understandable as follows. The neutron halo is formed since the orbital with a low angular momentum gains energy by extending the wave function. This effect is largest in the $s-$ orbital and next largest in the p orbital, concerning with the angular momentum barrier in the related effective potential term. Therefore a initiation for the rearrangement in nuclear orbitals emerges causing to a change in the shell structure. The diffuseness through the surface of the nucleus, with a striking large extension of the radius, results another variation in the spin–orbit interaction, as discussed through Section 2.1 in terms of the tensor interaction [39], which is vital to create the usual magic numbers beyond

N = 20. *The loose binding* and the *spread along the surface* rise subsequent *variations in pairing energy*. Figs. 7 (b) and (c) reveal that the pairing energy is functions of both the mass number and *neutron excess*, i.e. *isospin*.
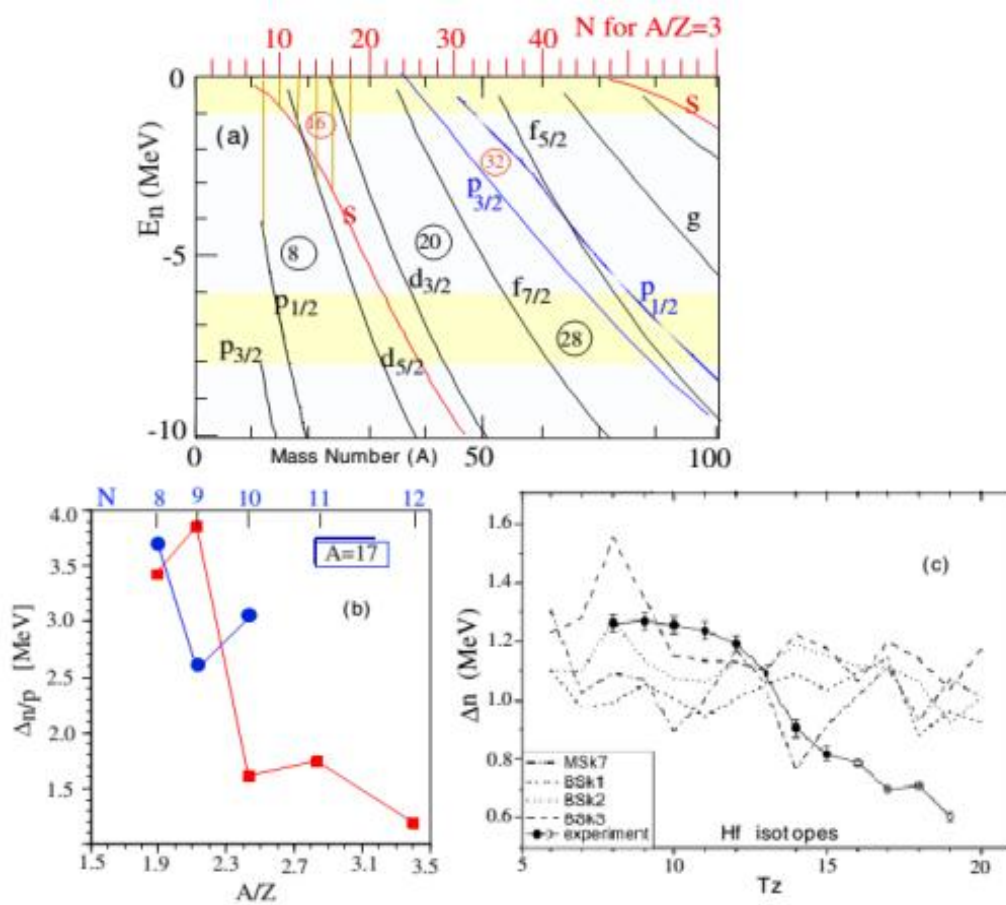

Fig.7. (a) Orbitals for neutral particles obtained by a Woods–Saxon potential [34]. (b) The neutron (squares) and proton (circles) pairing energies [36]. (c) Pairing energies for neutrons in Hf isotopes against isospin [37]. The pairing energies decrease with the increase in the n-p asymmetry.

Furthermore, moving toward an understanding of nuclei *at the threshold* of nuclear binding is an interesting research topic of contemporary nuclear physics. Along this line, in reviewing the data for light nuclei, Hoffman and his co-workers [40] have recently shown that the *binding energy plays a crucial role* in characterizing the variations in energy of *s*-states comparing to other states. Because the behavior of states with vanishing angular momentum within a few *MeV* of threshold is qualitatively different from that of neutron states with $\ell \geq 1$ or of any proton state. After an exhaustive work, the authors in [40] have concluded that the lingering of neutron *s*-states just below threshold is associated with the radial extension and consequently the diffuseness of the halo neutrons.

For the clarification of this point the researchers in [40] have proceeded with a specific region of atomic nuclei. In light stable nuclei the $0p$ shell closes with eight nucleons, accounting for the stability of ^{16}O. The $0d_{5/2}$ and $1s_{1/2}$ orbitals are close in binding energy in the vicinity of ^{16}O, but their spacing *increases substantially in lighter nuclei*, with the $5/2^+$ state moving more rapidly in excitation energy than the $1/2^+$ state. The $1/2^-$ state also moves rapidly with respect to the $1/2^+$ state. This is shown *for a subset of the experimental information* (nuclei with seven neutrons) in Fig. 8. In the present communication we focus on the behavior of the $1/2^+$ and $5/2^+$ single-neutron excitations. Through an examination of the simple geometrical *effects of finite binding*, Fig. 8 clarifies that it is the qualitatively different behavior of *neutron $s-$* states *near threshold* which *crucially* defines the sequence of levels in *weakly bound light nuclei*. To explore the changing pattern of states, one may examine the available data [40] where there is only one neutron in the $1s0d$ shell, spanning a range of neutron binding energies. We remind at this stage that the orbits with *small angular momentum* and *small binding energy* spend an *appreciable amount of time outside the nucleus* and thus benefit less from an increase in the size of the potential than do the loosely bound orbits with large ℓ.

Although, the behavior of $s-$ states near threshold has been commented on before, *none of these* discussions make mention of how successfully *finite binding effects* provide an explanation for the pattern of behavior observed in the data, unlike the work in [40].
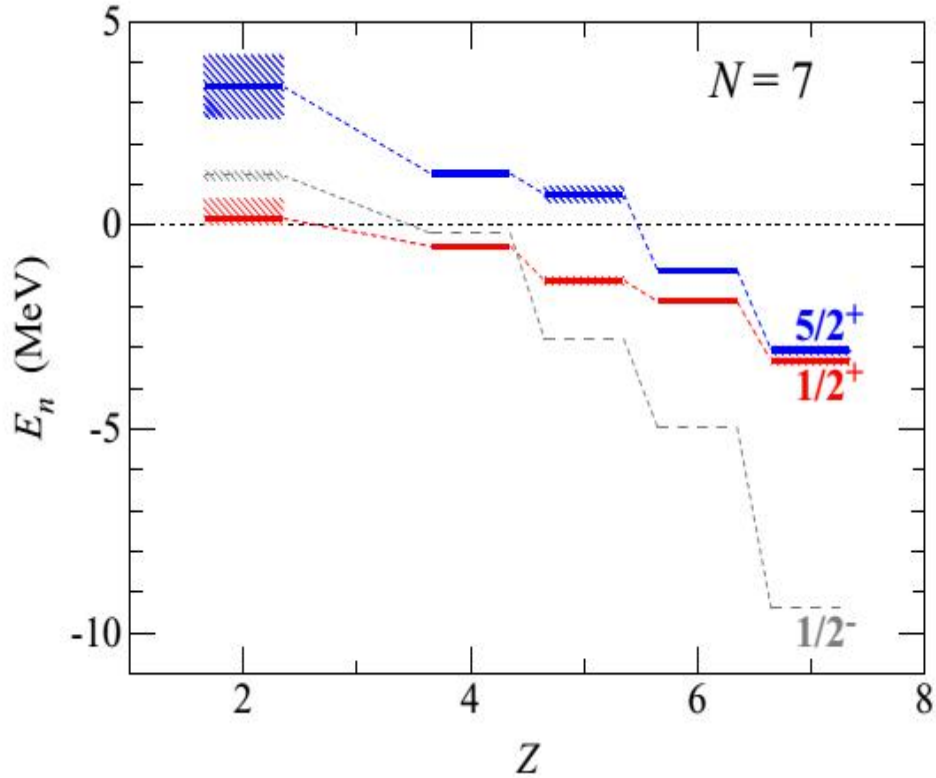
Fig. 8. The available observations on the energy relative to the threshold for neutrons for the $0p_{1/2}$, $1s_{1/2}$, and $0d_{5/2}$ states with $N = 7$ nuclei. Shadings denote uncertainties. Reprinted from [40].

As discussed in Section 2.1, the explicit recognition of the *tensor component* of the free *n-p* force and its monopole component has provided a successful explanation for many of the changes in magic numbers. *However*, based on the accumulated data presented in [40], *the magnitude of the observed effect seems considerably larger than can be accounted for by the tensor force.*

To examine the behavior of single nucleon states, the authors of [40] have used a Woods-Saxon potential form with reasonable radial parameters and calculated energy of the $0p_{1/2}$, $1s_{1/2}$, and $0d_{5/2}$ orbitals to plot these energies with respect to ΔV, where $\Delta V \equiv V - V_0$ with V_0 being the potential strength needed to put the energy of a specific orbital at threshold. The behavior of the neutron $1/2^+$ state near zero binding is quite dramatic:
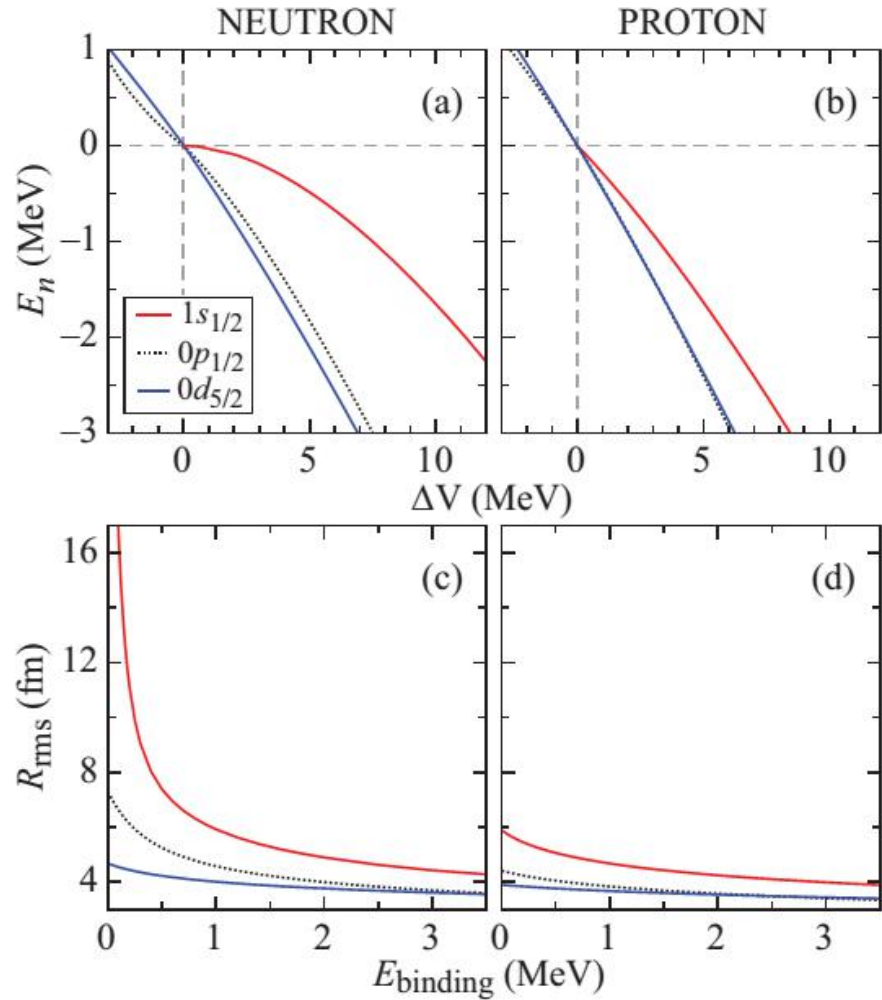
Fig. 9. Panels (a) and (b) illustrate theoretical calculations for $0p_{1/2}$, $1s_{1/2}$ and $0d_{5/2}$ where ΔV represents the change in potential strength around $E_n = 0$. Panels (c) and (d) show the related radii as a function of binding energies.

The same increment in the potential depth that increases the binding of the neutron $1/2^-$ and $5/2^+$ states from 0 to $1\,MeV$ causes a change in the $s-$state that is almost an order of magnitude less. This influence of the threshold is readily observed for the neutron $s-$state while it plays a much smaller role for $\ell \succ 0$ neutrons or for protons. The effect increases proportionally with an increase in *rms radius* of the neutron density distribution; in other words, diffuse halo states are prominently observed for *s-state* neutrons. In Fig. 9, the large increase in *rms radius* for neutron with $\ell = 0$ near threshold is evident when compared to those for protons or neutrons with $\ell \geq 1$. The present Woods-Saxon results, in the light of [40], suggest that this tendency of neutron $s-$states to linger just below threshold is a general property for neutrons with zero angular momentum.

Moreover, to explore the degree to which geometric effects play a role in the difference between the $1/2^+$ and $5/2^+$ excitations, the authors of [40] have also calculated the single-particle energies in a potential using a properly chosen Woods-Saxon shape. The results are illustrated in Fig. 10, together with those obtained experimentally.
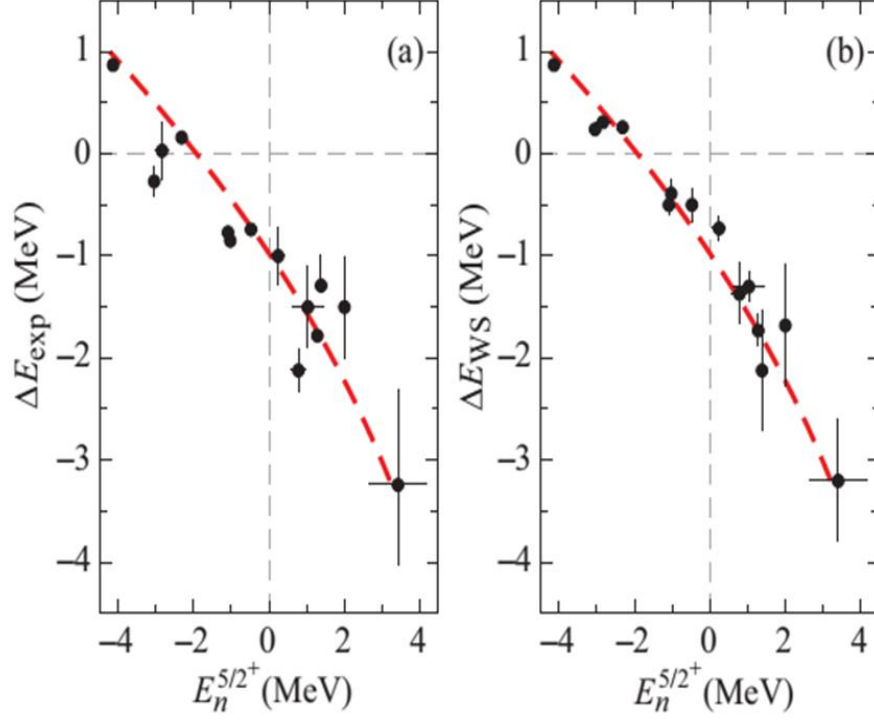
Fig. 10. (a) The experimental variation between states, $\Delta E_{\text{exp}} \equiv E_n^{1/2^+} - E_n^{5/2^+}$ (b) The same difference calculated in a Woods-Saxon potential. The dashed line is a smooth curve fit to the Woods-Saxon calculations and is the same in the two plots. Taken from [40].

From the comparison through Figs. 10 (a) and 10 (b), it is obvious that much of the variation in ΔE arises from finite binding effects. This is the dominant mechanism determining the ordering of the $1s_{1/2}$ and $0d_{5/2}$ orbitals in these nuclei.

The behavior of $s-$ wave neutrons near threshold is also the same physics responsible for the halo phenomenon, including neutron-pair halos such as in ^{11}Li. This is implicit in the discussions of Refs. [41]. The tendency for these $s-$ states to stay around threshold also suggests that ground states with halos may occur over a relatively larger region of nuclei, as discussed through the report, than might be estimated otherwise.

CHAPTER 4

CONCLUDING REMARKS

Over the last two decades our knowledge about nuclear structure has expanded tremendously due to the search for exotic unstable nuclei. This reveals considerable modification of the shell structure when one moves the neutron-rich dripline region. Along this line, recently, Ozawa and his co-workers have clearly shown the existence of a new neutron magic number $N = 16$ [34] from a systematic study of the single-neutron separation energies in neutron-rich halo nuclei. These observations suggest the possibility of the change of shell closures in a wide range of neutron-rich nuclei. Within this context, *in the first part of the present report*, the *magic numbers in exotic nuclei* has been discussed and their novel origin has been shown, within the frame of the related literature, to be the *spin-isospin* dependent part of the nucleon-nucleon interaction in nuclei. The finding of *new* magic numbers would also of immense astrophysical interest.

Secondly, we have presented the considerable impact of *3N forces* on the spectra of *neutron-rich oxygen isotopes* as such isotopes provide an exciting laboratory, both experimentally and theoretically, to study the structure of extreme neutron-rich nuclei towards and beyond the neutron dripline at ^{24}O. We have argued that the use of a *proper 3N mechanism* as mentioned in Refs. [19,25] yields *repulsive interactions* between valence nucleons. Employing sophisticated microscopic calculations for interacting nucleons, including three-body forces, together with the known single particle energies, the corresponding theoretical shell model calculations explain explicitly why ^{24}O is the *heaviest oxygen isotope*.

Finally, we have focussed at the recent study [40] of data on the $1s_{1/2}$ and $0d_{5/2}$ states in light neutron-rich halo nuclei to understand the *critical effect of binding energy* on the notable trend in the separation of these orbitals as shown in Fig.8. Over a relatively small range of neutron excess, between isotopes of He and O, the states diverge by around $4\,MeV$. Through the work in Ref. [40] it has been shown that a significant fraction of this deviation can be attributed to the behavior of the neutron $s-$ state *near threshold*, *leading to a dominant* geometric effect of *finite binding*, with the action of the *tensor force* laying only *a small role*.

Light exotic nuclei, like the ones discussed in the present report, with one or two weakly bound neutrons in their halo offer the opportunity to study large systems at small nuclear density. Along this line the works are in progress.

REFERENCES

[1] Tanihata I *et al* 1985. Measurements of interaction cross-sections and radii of He isotopes. *Phys. Lett. B* **160** 380

[2] Tanihata I *et al* 1985.Measurements of interaction cross-sections and nuclear radii in the light p-shell region**.** *Phys. Rev. Lett.* **55** 2676

[3] Hansen P G and Jonson B 1987. The neutron halo of extremely neutron-rich nuclei. *Europhys. Lett.* **4** 409; Jensen A S and Riisager K 2000. Towards necessary and sufficient conditions for halo occurence. *Physics Lett. B* **480 3**9

[4] Bertulani C A, Canto L F and Hussein M S 1993. The structure and reactions of neutron-rich nuclei**.** *Phys. Rep.* **226** 281

[5] Zhukov M V *et al* 1993. Bound state properties of Borromean halo nuclei He-6 and Li-11**.** *Phys. Rep.* **231** 151

[6] Riisager K 1994. Nuclear halo states. *Rev. Mod. Phys*. **66** 1105

[7] Tanihata I 1995. Nuclear structure studies from reaction induced by radioactive nuclear beam. *Prog. Part. Nucl. Phys*. **35** 505

[8] Hansen P G, Jensen A S and Jonson B 1995. Nuclear halo. *Annu. Rev. Nucl. Part. Sci*. **45** 591

[9] Tanihata I 1996. Neutron halo nuclei. J. Phys. G: *Nucl. Part. Phys.* **22** 157

[10] Jonson B and Riisager K 1998. Halo and halo excitations. *Phil. Trans. R. Soc. A* **356** 2063

[11] Jensen A S and Zhukov M V 2001. Few-body effects in nuclear halos. *Nucl. Phys. A* **693** 411

[12] Jonson B 2004. Light dripline nuclei. *Phys. Rep*. **389** 1

[13] Jensen A S, Riisager K, Fedorov D V and Garrido E 2004. Structure and reactions of quantum halos. *Rev. Mod. Phys.* **76** 215

[14] Riisager K 2006 The Euroschool Lectures on Physics with Exotic Beams. Nuclear halos and experiments to probe them. (*Lectures on Physics 700 vol II)* (Heidelberg: Springer) p 1

[15] Riisager K 2013. Halo and related structures. *Phys. Scr.* ***T*152** 014001

[16] Frederico T, Delfino A, Tomio L and Yamashita M T 2012. Universal aspects of light halo nuclei. *Prog. Part. Nucl. Phys.* **67** 939

[17] Goeppert Mayer M 1949. On close shells in nuclei.II. *Phys. Rev.* **75** 1969; Goeppert Mayer M 1950. Nuclear configurations in the spin-orbit coupling model.I. Empirical evidence. *Phys. Rev.* **78** 16

[18] Haxel O, Jensen J H D and Suess H E 1949. On the magic numbers in nuclear structure. *Phys. Rev.* **75** 1766

[19] Otsuka T 2013. Exotic nuclei and nuclear forces. *Phys. Scr.* ***T*152** 014007

[20] Bansal R K and French J B 1964. Even-parity hole states in $f_{7/2}$ shell nuclei. Phys. Lett. **11** 145; Poves A and Zuker A 1981. Theoretical spectroscopy and the *fp* shell. *Phys. Rep.* **70** 235

[21] Otsuka T et al 2001. Magic numbers in exotic nuclei and spin-isospin properties of the nucleon-nucleon interaction. *Phys. Rev. Lett*. **87** 082502

[22] Otsuka T 2002. Shell, shape and spin-Isospin structures of exotic nuclei. *Prog. Theor. Phys. Suppl.* **146** 6

[23] Wiringa R B, Pieper S C, Carlson J and Pandharipande V R 2001. Realistic models of pion-exchange three-nucleon interactions. *Phys. Rev. C* **62** 014001

[24] Otsuka T, Suzuki T, Fujimoto R, Grawe H and Akaishi Y 2005. Evolution of nuclear shells due to the tensor force. *Phys. Rev. Lett.* **95** 232502

[25] Otsuka T, Suzuki T, Holt J, Schwenk A and Akaishi Y 2010. Three body forces and the limit of oxygen isotopes. *Phys. Rev. Lett.* **105** 032501

[26] Guillemaud-Mueller D *et al* 1990. Particle stability of the isotopes ^{26}O and ^{32}Ne in the reaction 44 MeV/nucleon ^{48}Ca +Ta. *Phys. Rev. C* **41** 937; Fauerbach M *et al* 1996. New search for ^{26}O. *Phys. Rev. C* **53** 647

[27] Janssens R V F 2009. Unexpected double magic nucleus. *Nature* **459** 1069; Ozawa A *et al* 2000. A new magic number N=16 near to the neutron dripline. *Phys. Rev. Lett.* **84** 5493; Hoffman C R *et al* 2008. Determination of the N=16 shell closure at the oxygen dripline. *Phys. Rev. Lett.* **100** 152502; Kanungo R *et al* 2009. One-neutron removal measurement reveals ^{24}O as a new double magic nucleus. *Phys. Rev. Lett.* **102** 152501

[28] Hjorth-Jensen M, Kuo T T S and Osnes E 1995. Realistic effective interactions for nuclear systems. *Phys. Rep.* **261** 125

[29] Bogner S K, Kuo T T S and Schwenk A 2003. Model independent low momentum nucleon interaction from phase shift equivalence. *Phys. Rep.* **386** 1; Bogner S K *et al* 2007. Low momentum interactions with smooth cutoffs. *Nucl. Phys. A* **784** 79

[30] Utsuno Y, Otsuka T, Mizusaki T and Honma M 2004. Onset of intruder ground state in exotic Na isotopes and evolution of the N=20 shell gap. *Phys. Rev. C* **70** 044307

[31] Brown B A and Richter W A 2006. New ''USD'' Hamiltonians for the sd-shell. *Phys. Rev. C* **74** 034315

[32] Bogner S K *et al* 2009. Nuclear matter from chiral low-momentum interactions. *arXiv:*0903.3366 *[nucl-th]*

[33] Zuker A P 2003. Three body monopole corrections to realistic interactions. *Phys. Rev. Lett.* **90** 04250

[34] Ozawa A *et al* 2000. New magic number N=16, near the neutron dripline. *Phys. Rev. Lett.* **84** 5493; Hoffman C R *et al* 2008. Determination of the N=16 shell closure at the oxygen dripline. *Phys. Rev. Lett.* **100** 152502; Kanungo R *et al* 2009. One neutron measurement reveals ^{24}O as a new double magic nucleus. *Phys. Rev. Lett.* **102** 152501

[35] Bohr A and Mottelson B R 2008. The development of concepts in nuclear physics. *Nucl. Struct.* **1** 169

[36] Kanungo R 2003. Nuclear shell change as the limit of stability. *Nucl. Phys. A* **722** 30c

[37] Litvinov Y *et al* 2005. Isospin dependence in the odd-even staggering of nuclear binding energies. *Phys. Rev. Lett.* **95** 042501

[38] Pieper C and Wiringa R B 2001. Quantum monte carlo calculations of light nuclei. *Annu. Rev. Nucl. Part. Sci.* **51** 53

[39] Tanihata I 2013. Effects of tensor forcs in nuclei. *Phys. Scr.* ***T*152** 014021

[40] Hoffman C R, Kay B P and Schiffer J P 2014. Neutron s-states in loosely bound nuclei. *Phys. Rev. C* **89** 61305 (R)

[41] Hamamoto I and Mottelson B. R 2003. A personal view of some issues involved in the structures of nuclei with large neutron excess. *C. R. Phys.* **4**, 433; Tanihata I, Savajols H, and Kanungo R 2013. Recent progress in halo studies: Progress in particle and nuclear physics. *Prog. Part. Nucl. Phys.* **68**, 215

APPENDIX A

REMARKS ON THE NUCLEAR INTERACTIONS

Many nuclear structure models exist to describe the properties of the nuclei as quoted through the present report. One can ask why is there so many models rather than a unique one? Reasons are both practical and phenomenological. From the practical point of view, the most fundamental approach, which would treat the nucleus as interacting fermions by means of short range forces, is often intractable due to the difficulties for the treatment of the corresponding many-body problem exactly in a plausible analytical form. On the phenomenological side, the nucleus explores different degrees of freedom, ranging from the spherical magic, the deformed or cluster shapes, the one or two nucleon halos, to the particle-unbound systems. It is an extremely changeable system, which is also making the field of nuclear structure so diverse and fascinating. But it is tempting and often wise to use models which are suitable to describe one or few of these observed phenomena in a proper approximate form.

From all these model calculation results, a brief summary of the most important features of the nucleon-nucleon interaction in nuclear matter are presented as follows.

- The nuclear interaction is of short range, of the order of a few fm.
- The nearly identical spectra for mirror nuclei suggest that the nuclear force is charge symmetric i.e. the proton-proton and neutron-neutron interactions are equal.

- In addition, because of the Pauli principle, two like nucleons in the same orbit cannot have identical quantum numbers, so two-neutron or two-proton configurations only exist in the S = 0 total spin state, as a S = 1 state would imply that both nucleons have the same spin projection. However, the nuclear force binds only this S = 1 state to form the ground state of the deuteron that is the only bound n-p system, unlike the other unbound nucleon configurations such as di-neutron and di-proton. This binding of the n-p configuration interestingly cannot be observed for S=0 case as the corresponding interaction potential strength is not enough to bound the related nucleon-nucleon system unlike the S=1 case mentioned above. This remarkable feature implies that the nuclear interaction is also spin dependent.

- The nuclear interaction has a spin-orbit component. A decisive step in the development of the nuclear shell model was the recognition that the assumption of a relatively strong spin-orbit interaction in the nucleonic motion leads to a naturel explanation of the major shell closures at 28, 50, 82, and 126 [17]. This component provokes a large splitting in energy between any two levels having the same orbital momentum ℓ with aligned or anti-aligned intrinsic spins. The aligned configuration, $j = \ell + 1/2$, is energetically favored, whereas the anti-aligned one, $j = \ell - 1/2$, is at a higher energy, which cause the energy splitting such as the $p_{1/2}$, $p_{3/2}$ and $d_{3/2}$, $d_{5/2}$ energy levels as shown below,
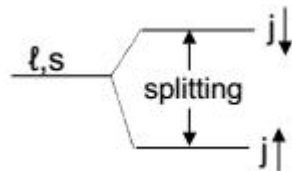
- Significant properties of the NN forces such as those of the central, spin-orbit and tensor terms prevail in the atomic nucleus, as witnessed by considerable modifications of shell structure. The more general potentials between two nucleons depend on three vector coordinates of the radius, spin and isospin as,

$$V(1,2) = V\left(\bar{r}_1, \bar{\sigma}_1, \bar{\tau}_1; \bar{r}_2, \bar{\sigma}_2, \bar{\tau}_2\right) \tag{A.1}$$

Following the general discussion in Chapter 2, the nucleon-nucleon interaction can be expanded in two main parts which are central and non-central. Using the spin-isospin representation, the central interaction is decomposed in four terms,

$$V_c(1,2) = V_0(r) + V_\sigma(r)\bar{\sigma}_1.\bar{\sigma}_2 + V_\tau(r)\bar{\tau}_1.\bar{\tau}_2 + V_{\sigma\tau}(r)\bar{\sigma}_1.\bar{\sigma}_2\,\bar{\tau}_1.\bar{\tau}_2 \tag{A.2}$$

where $r\left(=\bar{r}_1 - \bar{r}_2\right)$ is the distance between two nucleons. The non-central interaction contains two terms, (i) the two-body spin-orbit interaction given by

$$V_{LS}(1,2) = \left(V_{LS}^{is}(r) + V_{LS}^{iv}(r)\bar{\tau}_1.\bar{\tau}_2\right)\bar{L}.\bar{S} \tag{A.3}$$

where $\bar{L}$ is the relative orbital momentum between the two interacting nucleons, $\bar{S}$ is their total intrinsic spin being with $\bar{S} = \dfrac{1}{2}\left(\bar{\sigma}_1 + \bar{\sigma}_2\right)$ and the superscript is and iv hold for iso-scalar and iso-vector part of the potential. (ii) Whereas, the tensor part is defined by

$$V_T(1,2) = \left(V_T^{is}(r) + V_T^{iv}\bar{\tau}_1.\bar{\tau}_2\right)S_{12}(r) \tag{A.4}$$

where

$$S_{12}(r) = \frac{3}{r^2}\left(\bar{\sigma}_1.\bar{r}\right)\left(\bar{\sigma}_2.\bar{r}\right) - \bar{\sigma}_1.\bar{\sigma}_2 \tag{A.5}$$

The all realistic nucleon-nucleon interaction potentials published by the related literature, some of which are quoted in this report through Chapters 2 and 3, chose various forms for the eight functions appeared in Eqs. (A.2-A.5) according to specific problems considered. Chapter 2, as the heart of the present thesis work, has focused in particular the tensor part of the nuclear force, instead of its central and spin pieces, to justify the dominant effect of such monopole interaction on the shell evolution for halo nuclei.

APPENDIX B

WOODS-SAXON POTENTIAL

The Woods-Saxon potential is a convenient phenomenological choice for the one-body potential. It provides a model for the properties of bound-state and continuum single-particle wave-functions. The Woods-Saxon potential (or any other one-body potential) cannot be used for the total binding energy since it is not based upon a specific two-body interaction. The parameters of the Woods-Saxon are chosen for a best fit of nuclear single-particle energies and nuclear radii. The Woods-Saxon potential is based upon the sum of a spin-independent central potential, a spin-orbit potential, and the Coulomb potential similar to Eq. (A-3) for spherical nuclei,

for spherical nuclei,

$$V(r) = V_0(r) + V_{SO}(r)\,\vec{\ell}\cdot\vec{s} + V_C(r)\,, \qquad (B-1)$$

where $V_o(r)$ is the spin-independent central potential:

$$V_o(r) = V_o f_o(r)\,, \qquad (B-2)$$

with a fermi shape

$$f_o(r) = \frac{1}{1 + \left[\exp(\,r - R_0\,)/a_0\right]}\,, \qquad (B-3)$$

$V_{so}(r)$ is the spin-orbit potential:

$$V_{so}(r) = V_{so}\,\frac{1}{r}\,\frac{df_{so}(r)}{dr}\,, \qquad (B-4)$$

with

$$f_{so}(r) = \frac{1}{1 + \left[\exp(r - R_{so}) / a_{so}\right]}$$

(B-5)

and $V_C(r)$ is the Coulomb potential for protons based upon the Coulomb potential for a sphere of radius R_c ,

$$V_C(r) = \frac{Ze^2}{r} \quad \text{for} \quad r \geq R_c$$

and $$V_C(r) = \frac{Ze^2}{R_c}\left[\frac{3}{5} - \frac{r^2}{2R_c^2}\right] \quad \text{for} \quad r \leq R_c$$

(B-6)

The radius R_o , R_{so} and R_c are usually expressed as :

$$R_i = r_i A^{1/3}.$$

(B-7)

For nuclei with a neutron excess the protons will feel a stronger potential than the neutrons, since the average proton-neutron potential is stronger than the average neutron (or proton-proton) potential. Thus we take:

$$V_{0p} = V_0 + \frac{(N - Z)}{A}V_1 \qquad \text{for protons}$$

(B-8)

$$V_{0n} = V_0 - \frac{(N - Z)}{A}V_1 \qquad \text{for neutrons}$$

(B-9)

In principle, r_0 and a_0 could also be a little difference for proton and neutrons in a nucleus with $N \neq Z$. Thus the spin-indepedent potential could have six parameters (and even more is any of them are allowed to take some additional mass dependence). The values of these parameters are chosen to give an overall accounting of the observed single-particle energies, the rms charge radii, and the electron scattering form factors.